



Contents lists available at ScienceDirect

Nuclear Instruments and Methods in Physics Research A

journal homepage: www.elsevier.com/locate/nima

The n_TOF Total Absorption Calorimeter for neutron capture measurements at CERN

C. Guerrero^{a,*}, U. Abbondanno^b, G. Aerts^c, H. Álvarez^d, F. Álvarez-Velarde^a, S. Andriamonje^c, J. Andrzejewski^e, P. Assimakopoulos^f, L. Audouin^g, G. Badurek^h, P. Baumann^g, F. Bečvářⁱ, E. Berthoumieux^c, F. Calviño^j, M. Calviani^k, D. Cano-Ott^a, R. Capote^{m,ae}, C. Carrapiço^{c,ag}, P. Cennini^l, V. Chepelⁿ, E. Chiaveri^l, N. Colonna^o, G. Cortes^j, A. Couture^p, J. Cox^p, M. Dahlfors^l, S. David^g, I. Dillmann^q, C. Domingo-Pardo^r, W. Dridi^c, I. Duran^d, C. Eleftheriadis^s, L. Ferrant^g, A. Ferrari^l, R. Ferreira-Marquesⁿ, K. Fujii^b, W. Furman^t, I. Goncalvesⁿ, E. González-Romero^a, F. Gramegna^k, F. Gunsing^c, B. Haas^g, R. Haight^u, M. Heil^v, A. Herrera-Martinez^l, M. Igashira^w, E. Jericha^h, F. Käppeler^v, Y. Kadi^l, D. Karadimos^f, M. Kerveno^g, P. Koehler^x, E. Kossionides^y, M. Krtičkaⁱ, C. Lampoudis^{c,s}, H. Leeb^h, A. Lindoteⁿ, I. Lopesⁿ, M. Lozano^{ae}, S. Lukic^g, J. Marganec^e, S. Marrone^o, T. Martínez^a, C. Massimi^z, P. Mastinu^k, E. Mendoza^a, A. Mengoni^{l,m}, P.M. Milazzo^b, C. Moreau^b, M. Mosconi^v, F. Nevesⁿ, H. Oberhummer^h, S. O'Brien^p, J. Pancin^c, C. Papachristodoulou^f, C. Papadopoulos^{aa}, C. Paradela^d, N. Patronis^f, A. Pavlik^{ab}, P. Pavlopoulos^{ac}, L. Perrot^c, M.T. Pigni^h, R. Plag^v, A. Plompen^{ad}, A. Plukis^c, A. Poch^j, J. Praena^k, C. Pretel^j, J. Quesada^{ae}, T. Rauscher^{af}, R. Reifarth^u, C. Rubbia^l, G. Rudolf^g, P. Rullhusen^{ad}, J. Salgado^{ag}, C. Santos^{ag}, L. Sarchiapone^l, I. Savvidis^s, C. Stephan^g, G. Tagliente^o, J.L. Tain^r, L. Tassan-Got^g, L. Tavora^{ag}, R. Terlizzi^o, G. Vannini^z, P. Vaz^{ag}, A. Ventura^{ah}, D. Villamarin^a, M.C. Vicente^a, V. Vlachoudis^l, R. Vlastou^{aa}, F. Voss^v, S. Walter^v, M. Wiescher^p, K. Wisshak^v

^a Centro de Investigaciones Energeticas Medioambientales y Tecnológicas, Madrid, Spain

^b Istituto Nazionale di Fisica Nucleare, Trieste, Italy

^c CEA/Saclay – DSM/DAPNIA, Gif-sur-Yvette, France

^d Universidade de Santiago de Compostela, Spain

^e University of Lodz, Lodz, Poland

^f University of Ioannina, Greece

^g Centre National de la Recherche Scientifique/IN2P3-IReS, Strasbourg, France

^h Atominstytut der Österreichischen Universitäten, Technische Universität Wien, Austria

ⁱ Charles University, Prague, Czech Republic

^j Universidad Politecnica de Catalunya, Spain

^k Istituto Nazionale di Fisica Nucleare (INFN), Laboratori Nazionali di Legnaro, Italy

^l CERN, Geneva, Switzerland

^m International Atomic Energy Agency (IAEA), Nuclear Data Section, Vienna, Austria

ⁿ LIP – Coimbra and Departamento de Fisica da Universidade de Coimbra, Portugal

^o Istituto Nazionale di Fisica Nucleare, Bari, Italy

^p University of Notre Dame, Notre Dame, USA

^q Physik-Department E12, Technische Universität München, Garching, Germany

^r Instituto de Fisica Corpuscular, CSIC-Universidad de Valencia, Spain

^s Aristotle University of Thessaloniki, Greece

^t Joint Institute for Nuclear Research, Frank Laboratory of Neutron Physics, Dubna, Russia

^u Los Alamos National Laboratory, NM, USA

^v Forschungszentrum Karlsruhe GmbH (FZK), Institut für Kernphysik, Germany

^w Tokyo Institute of Technology, Japan

^x Oak Ridge National Laboratory, Physics Division, Oak Ridge, USA

^y NCSR, Athens, Greece

^z Dipartimento di Fisica, Università di Bologna, and Sezione INFN di Bologna, Italy

^{aa} National Technical University of Athens, Greece

^{ab} Institut für Isotopenforschung und Kernphysik, Universität Wien, Austria

^{ac} Pôle Universitaire Léonard de Vinci, Paris La Défense, France

^{ad} CEC-JRC-IRMM, Geel, Belgium

^{ae} Universidad de Sevilla, Spain

^{af} Department of Physics - University of Basel, Switzerland

^{ag} Instituto Tecnológico e Nuclear (ITN), Lisbon, Portugal

^{ah} ENEA, Bologna, Italy

* Corresponding author. Tel.: +34 913466778; fax: +34 913466576.

E-mail address: carlos.guerrero@ciemat.es (C. Guerrero).

ARTICLE INFO

Article history:

Received 30 June 2009

Accepted 20 July 2009

Keywords:

n_TOF

Neutron capture

Neutron cross-sections

Total Absorption

Time-of-Flight

BaF₂ detector

ABSTRACT

The n_TOF Collaboration has built and commissioned a high-performance detector for (n, γ) measurements called the Total Absorption Calorimeter (TAC). The TAC was especially designed for measuring neutron capture cross-sections of low-mass and/or radioactive samples with the accuracy required for nuclear technology and stellar nucleosynthesis. We present a detailed description of the TAC and discuss its overall performance in terms of energy and time resolution, background discrimination, detection efficiency and neutron sensitivity.

© 2009 Elsevier B.V. All rights reserved.

1. Introduction

The Total Absorption Calorimeter (TAC) is a segmented 4π detector array made of 40 BaF₂ crystals for neutron capture cross-section measurements at the CERN n_TOF Neutron Time-of-Flight Facility [1]. The high-efficiency detector in combination with long flight path of 185 m and high instantaneous neutron flux at n_TOF of 1.2×10^6 neutrons/pulse provides the opportunity for accurate neutron capture cross-section measurements on low-mass and/or radioactive samples for applications in nuclear technology [2–4] and stellar nucleosynthesis [5,6]. In the specific fields of accelerator driven systems (ADS) for transmutation of nuclear waste and of Generation-IV reactors, the need for more accurate cross-sections has been widely discussed [7], and many n_TOF measurements have already been funded by EC Framework Programs (n_TOF-NDADS [8], IP-EUROTRANS [9]) and other international projects.

At n_TOF, neutron capture cross-sections are measured using either a pair of C₆D₆ total energy detectors or the TAC. The first technique is based on low-efficiency, low-energy resolution detectors with an efficiency proportional to γ -ray energy [10]. The current version consists of C₆D₆ detectors, for which the required proportionality with γ -ray energy is achieved by the pulse height weighting technique [11,12]. This technique is also used for neutron capture measurements at GELINA [13], ORELA [14], and KURRI [15].

In contrast, the TAC is designed to detect the complete γ -ray cascade emitted in neutron capture reactions using detectors of high-intrinsic efficiency and large solid-angle coverage. By segmentation of the detector, the measured multiplicity can be combined with the deposited energy of a capture event for an improved background discrimination and for obtaining information on nuclear structure data characteristic of the compound nucleus [16].

The Total Absorption technique is best suited for measuring radioactive and/or small mass samples because of its high efficiency and background rejection capabilities. Large arrays of inorganic scintillators have therefore been built in the recent years for measuring neutron capture cross-sections, not only at n_TOF (40 BaF₂ crystals [17]), but also at other facilities such as FZK (41 BaF₂ crystals [27]), KURRI (4 π Ge [18] and 16 BGO crystals [19]), RPI (16 NaI crystals [20]) and LANL (162 BaF₂ crystals [21]).

In this work we describe the n_TOF TAC and discuss its overall performance in terms of energy and time resolution, background, detection efficiency and neutron sensitivity. The detector, the associated data acquisition system, and the samples for the first applications of the TAC are described in Section 2. Test measurements with γ -ray sources are presented in Section 3, and the performance in the first measurements of (n, γ) cross-sections of ¹⁹⁷Au and ²³⁷Np is discussed in Section 4, with particular emphasis on efficiency (Section 5) and neutron sensitivity (Section 6).

2. Experimental set-up

2.1. The n_TOF facility

At the n_TOF facility [1] neutrons are generated in spallation reactions by a pulsed 20 GeV proton beam impinging on a lead block, which is surrounded by 5 cm of water which serves as a coolant and as a moderator of the originally fast neutron spectrum. The resulting white neutron beam ranges from thermal energies to over 250 MeV with a nearly 1/E isoethargic flux dependence up to 100 keV. The neutrons travel through an evacuated beam line to the experimental area at a distance of 185.015(10) m from the spallation target. The intensity of the neutron beam in the experimental area is monitored by the *SiMon* system [22], an assembly of four silicon detectors facing a thin ⁶Li foil which intersects the neutron beam.

The experimental program at n_TOF includes measurements of fission cross-sections performed with Parallel Plate Avalanche Counters (PPAC) [23] and a Fast Induction Chamber (FIC) [24] and of capture cross-sections studied either with total energy detectors (C₆D₆) [25] or with the TAC described in this paper.

An overview of the n_TOF facility and the various measuring devices is given in Ref. [26] and further details can be found in Ref. [1].

2.2. The Total Absorption Calorimeter

The n_TOF TAC is based on the BaF₂ calorimeter built at Forschungszentrum Karlsruhe [27] and was designed to meet the requirements of an ideal Total Absorption detector: large solid angle coverage, high total γ -ray efficiency, good energy resolution, high segmentation, low neutron sensitivity and fast time response.

The TAC consists of 40 BaF₂ crystals, 12 pentagonal and 28 hexagonal in shape, which cover 95% of 4π . Both types of crystals are cut from BaF₂ cylinders 1 cm in diameter and 15 cm thickness with raw and final weights of 12 and 7.5 kg, respectively. For optimal light collection each crystal is covered with two layers of 0.1 mm thick Teflon foil and a 0.1 mm thick polished aluminum sheet on the outside. The crystals are put into 1 mm thick ¹⁰B loaded capsules and are coupled to an aluminum cylinder that houses also the 12.7 cm Photonis XP4508B photomultiplier. These individual detector modules are attached to an aluminum honeycomb structure, which holds the complete assembly. The TAC is divided into hemispheres that can be moved to open the detector for access to the samples in the center. Fig. 1 shows a picture of the open TAC with the neutron absorber surrounding the samples. Details of design, construction, and assembling of the TAC can be found in Ref. [28].

One of the main sources of background in (n, γ) measurements with the TAC is related to the capture of neutrons scattered in the

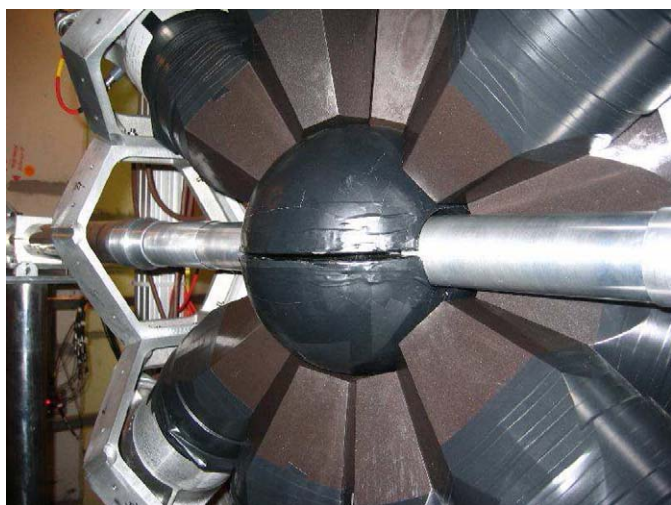


Fig. 1. View of one of the TAC hemispheres with the neutron absorber in the center and the neutron beam line.

sample. This background follows the same energy dependence as the true capture events and may therefore jeopardize the analysis of resonances. The probability for detecting such background events is referred to as the neutron sensitivity of the system. In the case of the TAC, this was reduced by combining the spherical neutron moderator/absorber surrounding the sample with the ^{10}B loaded (16% in mass) carbon fiber capsules of the crystals.

The neutron absorber material was selected by Monte Carlo simulations [30,29], which confirmed that the best neutron moderator/absorber combination is ^6LiH [21], which has the additional advantage of a very low γ -ray interaction cross-section thanks to its low effective atomic number Z . However, safety rules at CERN prohibit the use of ^6LiH due to its high flammability and toxicity, and therefore an inert non-flammable lithium salt $\text{C}_{12}\text{H}_{20}\text{O}_4(^6\text{Li})_2$ [29] was used instead. For stability, the compound was encapsulated in a spherical 0.5 mm thick aluminum shell with inner and outer radii of 5 and 10 cm, respectively. The absorber inside the TAC is shown in Fig. 1.

2.3. Samples

The samples used in a first series of TAC measurements were disks 1 cm in diameter. Stable samples were sandwiched between two Kapton foils and mounted in air between thin Kapton windows in the beam line. Radioactive samples had to be certified according to the ISO-2919 norm and were therefore sandwiched between two aluminum layers (<75 mg) and welded into titanium cans (~ 410 mg), as sketched in Fig. 2.

The data reported in this work refer to the TAC response to γ -rays from radioactive sources (^{137}Cs , ^{60}Co , ^{88}Y and ^{24}Na) and to (n, γ) reaction studies with stable (^{197}Au , graphite, and empty) samples; and with a radioactive (^{237}Np) sample. The measurements with the stable samples were performed to determine the ambient background (dummy-sample), the detection efficiency (^{197}Au), and the neutron sensitivity (graphite) of the TAC.

2.4. Data acquisition system

One of the main features of the experimental set-up at n_TOF is the fully digitized data acquisition system, which is described in detail in Ref. [31]. In particular, the BaF_2 signals are recorded by

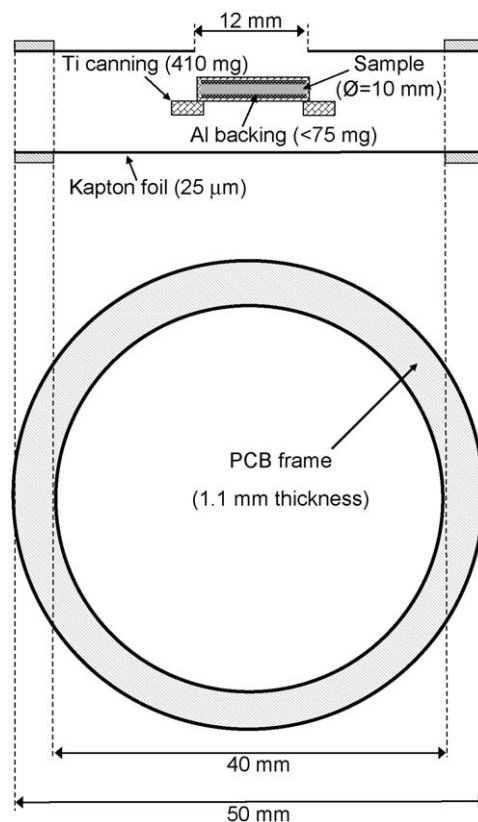


Fig. 2. Sketch of the sample assembly including titanium can and Kapton frame.

40 channels of high performance digitizers (Acqiris-DC270 [32]) with 8 bits resolution, 8 MB memory, and 500 MHz sampling rate. This system can record 16 ms long data buffers containing the digitized electronic response of each BaF_2 module for neutron energies between 0.3 eV and 20 GeV. A reduction in the sampling rate to 100 MSamples/s allows one to reach the $1/\nu$ energy region down to 0.028 eV.

After zero suppression and data formatting, the raw data are sent to CERN's massive CASTOR storage facility [33] via several Gigabit links. The raw data are stored in a temporary disk pool for on-line analysis and on magnetic tapes for repeated processing, thus providing the possibility for repeated investigations of systematic effects related to pile-up, γ/α discrimination, etc.

The digitized buffers are analyzed using a dedicated pulse shape analysis (PSA) routine for BaF_2 signals [34] that characterizes each signal by an analytic fit of the two components in the scintillation light ($\tau_{\text{fast}} = 0.7$ ns and $\tau_{\text{slow}} = 630$ ns). Fig. 3 shows an example of a digitized buffer containing five signals that are identified and reconstructed by the PSA routine.

The PSA routine extracts the relevant signal parameters for later data analysis, the Time-of-Flight (TOF), signal integral, and module identification number. This information is stored in data summary tapes, which are subsequently translated by coincidence analysis software into a list of detected events with a given neutron energy (E_n) calculated from the TOF, total deposited energy (E_{sum}) derived from the signal integral, and crystal multiplicity (m_{cr}) given by the number of modules involved in the detection of a capture of an event.

The existence of radium impurities in the crystals is responsible for a sizable α and β decay background that has been characterized experimentally (see Section 4.1). Signals produced by α -particles can be identified by the PSA routine because the

relative contributions of the fast and slow component of the light output depend strongly on the ionizing particle.

2.5. Measuring technique

By the TOF technique neutron cross-sections can be measured as a function of neutron energy. The technique is based on a

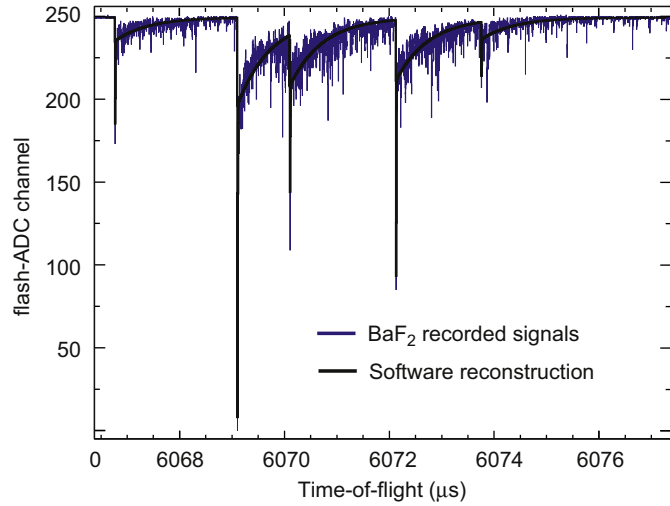


Fig. 3. Digitized buffer containing five BaF₂ signals that are identified and reconstructed by the PSA routine.

pulsed neutron source, where the energy of the neutron inducing a detected reaction is determined by

$$E_n(\text{eV}) = \left(\frac{72.2996 \cdot L(\text{m})}{t_{\text{det}}(\mu\text{s}) - t_0(\mu\text{s})} \right)^2 \quad (1)$$

where L is the distance between source and sample, and t_0 and t_{det} are the production and detection times, respectively. Note that this expression neglects relativistic effects and is, therefore, valid only below about 1 MeV.

Neutron capture reactions produce a cascade of several γ -rays with a total energy of $E_{\text{casc}} = S_n + (A/(A+1))E_n$, where A is the mass number of the isotope under study, S_n the neutron separation energy of the product nucleus, and E_n the energy of the incident neutron. The TAC is designed to absorb this cascade completely with efficiency as independent as possible from the decay scheme of the compound nucleus.

The observable quantity in (n, γ) measurements is the capture yield $Y_{n,\gamma}(E_n)$, which is the fraction of neutrons intersecting the sample undergoing a capture reaction. Experimentally, it is defined as

$$Y_{n,\gamma}(E_n) = \frac{C(E_n) - B(E_n)}{\varepsilon_{n,\gamma} N \Phi_n(E_n)}, \quad (2)$$

where $C(E_n)$ and $B(E_n)$ are the total and background count rates, $\varepsilon_{n,\gamma}$ the detection efficiency for capture cascades, $\Phi_n(E_n)$ the intensity of incident neutrons recorded by the SiMon system, and N the proportionality constant between the neutron intensity incident on the SiMon ($\varnothing = 3$ cm) and on the sample ($\varnothing = 1$ cm). For the purpose of this work, $N = 0.191(6)$ was calculated from the characterization of the neutron beam profile [43] and the

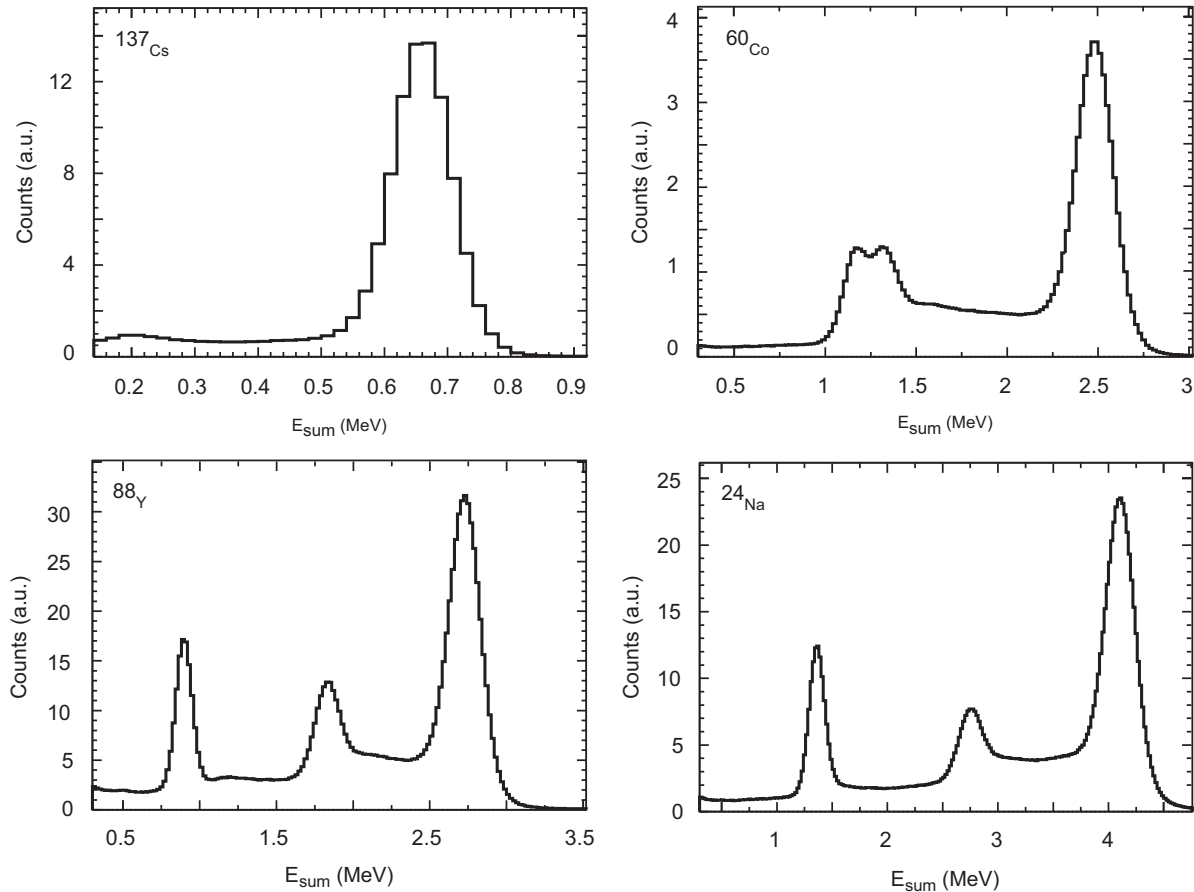


Fig. 4. TAC response to the standard γ -ray sources ¹³⁷Cs, ⁶⁰Co, ⁸⁸Y and ²⁴Na.

multiplicity, which can be classified according to their correlation with the neutron beam.

Backgrounds that are not correlated with the neutron beam are mainly due to the γ -ray activity of the radioactive samples with energies up to a few hundred keV, and to the radium impurities in the BaF₂ crystals with α and γ -ray energies up to a few MeV [27]. These backgrounds are characterized experimentally by dedicated *beam-off* measurements.

Backgrounds correlated with the neutron beam depend on neutron energy and also on the neutron capture and scattering cross-sections of the materials involved. These are mainly

- cascades from (n, γ) reactions in the sample canning and in beam line windows, and
- capture of neutrons scattered in the sample; taking the capture place in the neutron absorber, the ¹⁰B-loaded capsules, or in the Ba and F isotopes of the crystals.

These backgrounds have been characterized in dedicated runs. While the uncorrelated part was measured in *sample-out* runs, the backgrounds due to capture and scattering reactions in the sample assembly were determined in runs with a *dummy-sample* and with the *carbon scatterer*.

A last type of background that is dominant in measurement with Total Energy detectors at n_TOF, the in-beam γ -rays of 2.2 MeV caused by neutrons absorbed in the water moderator surrounding the spallation target, is just a negligible low energy background in the case of the TAC due to its high Total Absorption efficiency for capture cascades.

4.2. The reference case of ¹⁹⁷Au

The magnitude of background contributions is illustrated in the case of a real experiment with the 185 mg ¹⁹⁷Au sample. The comparison in Figs. 7 and 8 refers the measured deposited energy distributions in two energy intervals and the TOF spectrum between 1 eV and 30 keV. Such an upper limit corresponds to the energy above which the γ -flash of relativistic particles coming with the beam has a significant saturation effect on the electronics. The experimental distributions are normalized to the neutron beam intensity determined by the *SiMon* system in units of nominal proton pulses.

Fig. 7 shows the distributions of the deposited energy in the TAC (E_{sum}) for energy intervals from 1 to 10 eV (left) and from 1 to 10 keV (right). The contribution from capture reactions in ¹⁹⁷Au is

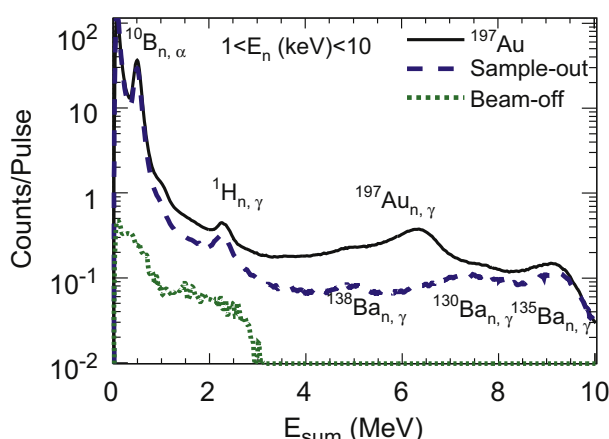
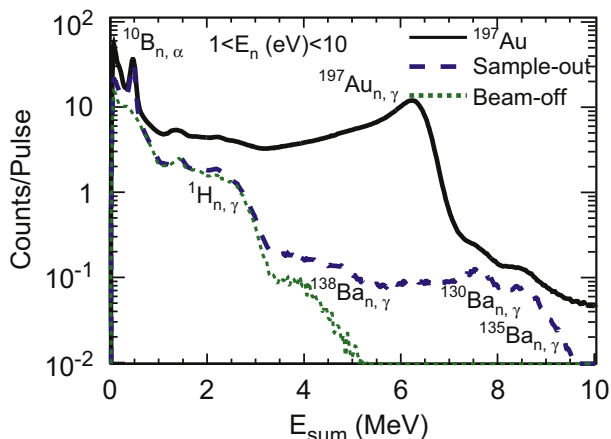


Fig. 7. Deposited energy distributions obtained with the 185 mg ¹⁹⁷Au sample and the related backgrounds in the neutron energy intervals from 1 to 10 eV (left) and from 1 to 10 keV (right).

limited to ~ 7.0 MeV, just above the neutron separation energy at $S_n(^{198}\text{Au}) = 6.54$ MeV; given that the summing of events due to pile-up is negligible. The main difference in the two E_n intervals is the magnitude of the background with respect to the capture reactions in ¹⁹⁷Au due to the relative energy dependency of the capture and scattering cross-sections of the indicated isotopes.

At low deposited energy, the *beam-off* measurement shows three components related to the β^- decay of radium and its progeny in the BaF₂ crystals [27]. The ²²⁶Ra decay chain yields a contribution of up to 3.2 MeV, while the ²²⁸Ra contribution ranges from 2.2 (²¹²Bi decay) to 5.0 MeV (²⁰⁸Tl decay). The peak at 1.46 MeV corresponds to ambient ⁴⁰K. The background from scattered neutrons along the beam line is characterized by the sample out measurement, which shows a peak at 0.478 MeV from the decay of ⁷Li* produced by (n, α) reactions in the ¹⁰B loaded capsules, a small structure at 2.2 MeV from ¹H(n, γ) reactions in the neutron absorber, and a high energy contribution from 4.7 to 9.1 MeV due to neutron captures in Ba and F. Events with deposited energies above 9.5 MeV indicate pile-up due to events overlapping within the 20 ns coincidence window.

Fig. 8 shows the TOF spectrum obtained in the three dedicated runs discussed before. The events were selected corresponding to

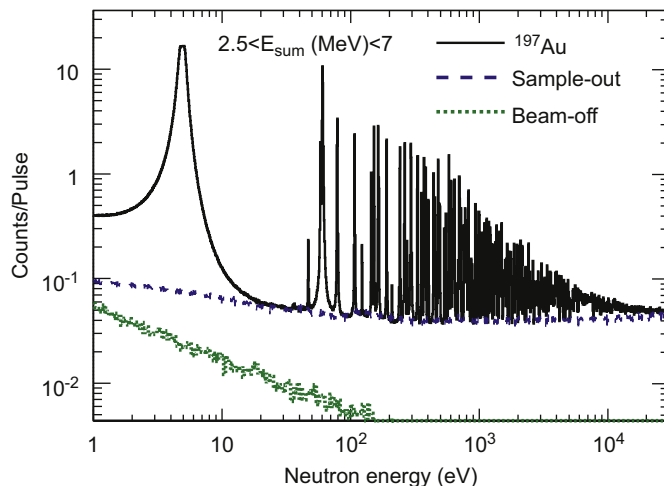


Fig. 8. Count rate distribution obtained with the ¹⁹⁷Au sample and backgrounds measured in dedicated runs with and without a dummy sample. Events were selected for deposited energies between 2.5 and 7 MeV, where the capture to background ratio is more favorable.

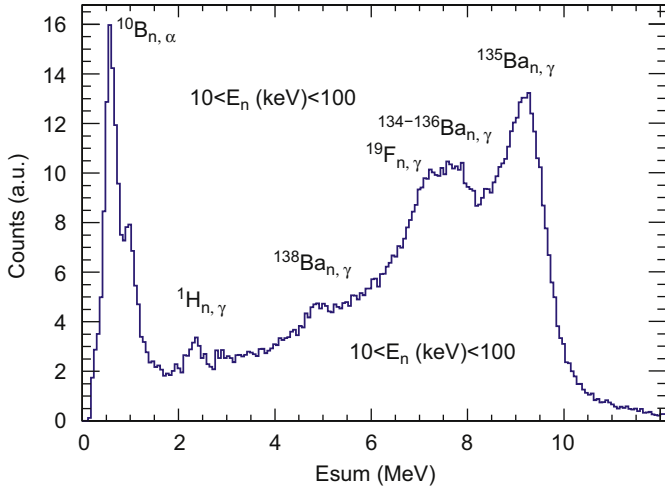


Fig. 11. Deposited energy distribution measured with a graphite sample for neutron energies between 10 and 100 keV.

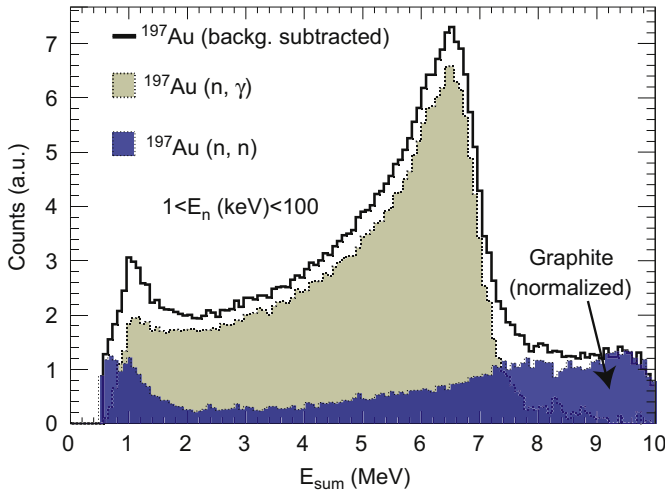


Fig. 12. Measured deposited energy distribution of ^{197}Au , separated into pure capture and scattering contributions for neutron energies between 1 and 100 keV and for the condition $m_{cr} > 2$.

The background reduction achieved by the m_{cr} condition is given in Fig. 13 for the $^{197}\text{Au}(n, \gamma)$ measurement. The three spectra shown correspond to the conditions $m_{cr} > 0$, $m_{cr} > 1$ and $m_{cr} > 2$. The low-energy background caused by the intrinsic γ -ray activity of the BaF_2 crystals and the 478 keV γ -ray following $^{10}\text{B}(n, \gamma)$ reactions is strongly reduced with $m_{cr} > 1$ and nearly eliminated with $m_{cr} > 2$. The background at the high-energy end of the spectrum, which is not much affected by either one of these conditions, can be eliminated by selecting an upper deposited energy threshold at 7 MeV.

The m_{cr} and E_{sum} conditions for the optimal capture to background ratio depend on the particularities of each measurement, e.g. on the radioactivity of the sample, the capture-to-scattering ratio, and the energy and average multiplicity of the capture cascades. For ^{197}Au , the best balance between background reduction and loss of efficiency was found for $m_{cr} > 2$ and $2.5 < E_{sum}(\text{MeV}) < 7$.

5. Detection efficiency

In principle, the large solid angle coverage and the 15 cm thick BaF_2 crystals result in a detection efficiency for capture events of

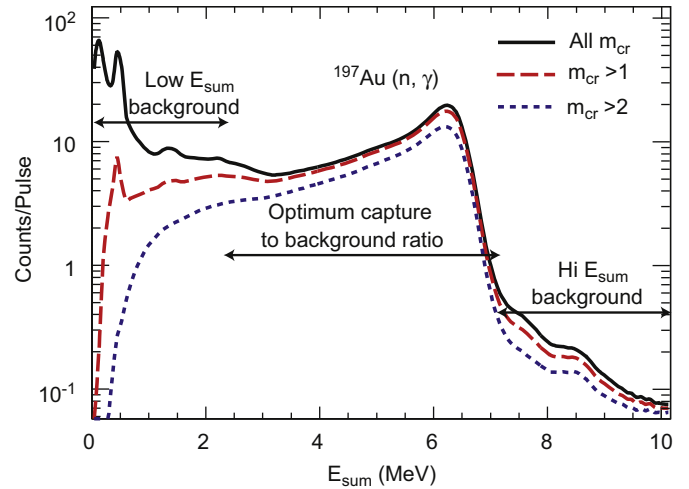


Fig. 13. Deposited energy distribution from the $^{197}\text{Au}(n, \gamma)$ measurement for different crystal multiplicities in the neutron energy interval from 1 to 10 eV.

almost 100%, regardless of the de-excitation pattern of the compound system under study. However, the efficiency of the TAC is reduced by the neutron absorber as well as by the conditions set for m_{cr} and E_{sum} . At high counting rates it is further affected by pile-up events as outlined in Ref. [36].

The detection efficiency can be determined experimentally for any condition on m_{cr} and E_{sum} by means of the saturated resonance method [39], where the theoretical and the observed capture yields are compared for a particular resonance that meets the following requirements:

1. The peak cross-section and the sample thickness must be large enough for the resonance to be saturated at the top: $(1 - e^{-n\sigma_{tot}}) \rightarrow 1$.
2. The capture to scattering cross-section ratio must be large enough so that the saturation point ($Y_{n,\gamma}^{sat} \sim \sigma_{\gamma} / (\sigma_{\gamma} + \sigma_n)$) can be determined accurately.

For this purpose we used the well-known resonance of ^{197}Au at 4.9 eV [39].

The theoretical capture yield of ^{197}Au in the vicinity of the 4.9 eV resonance was calculated with the SAMMY code [41], assuming the resonance parameters of the JEFF-3.1 cross-section library [42], i.e. $\Gamma_{\gamma} = 122.5$ meV and $\Gamma_n = 15.2$ meV. The SAMMY calculation includes all known experimental effects such as self-shielding, multiple-scattering, Doppler and resolution broadening. The observed capture yield

$$Y_{n,\gamma}^{obs}(E_n) = \frac{C(E_n) - B(E_n)}{N \cdot \Phi_n(E_n)} \quad (3)$$

is derived from measured quantities, which have already been defined in Eq. (2).

The ^{197}Au capture yields with the saturated region between 4.7 and 5.1 eV are shown in Fig. 14 for different conditions. The lines are the theoretical yields scaled to match the experimental yields. The detection efficiency of the TAC for capture reactions on ^{197}Au is given by the respective scaling factor.

The detection efficiencies obtained in this way are listed in Table 1. Obviously, efficiency is reduced as the conditions become more restrictive. The quoted uncertainties are only determined by the accuracy of the SAMMY fit ($< 1\%$), the saturation level of the resonance calculated with the evaluated cross-section from the

Radioactivos de Alta Actividad and by the European Commission 5th Framework Programme under Contract number FIKW-CT-2000-00107 (n_TOF-ND-ADS Project).

References

- [1] The n_TOF Collaboration, CERN n_TOF facility: performance report, CERN/INTC-O-011, INTC-2002-037 CERN-SL-2002-053 ECT, 2006.
- [2] W. Gudowski, Nucl. Phys. A 654 (1999).
- [3] G. Aliberti, et al., Nucl. Sci. Eng. 146 (2004) 13.
- [4] J. Bouchard, Nuclear data for innovative reactors and fuel cycles, in: Proceedings of the International Conference on Nuclear Data for Science and Technology, vol. 718, Nice, France, 2007.
- [5] G. Wallerstein, et al., Rev. Mod. Phys. 69 (1997) 995.
- [6] M. Arnould, From the microcosm of the atomic nuclei to the macrocosm of the stars, in: Proceedings of the International Conference on Nuclear Data for Science and Technology, vol. 712, Nice, France, 2007.
- [7] NEA/WPEC-26, Uncertainty and target accuracy assessment for innovative systems using recent covariance evaluations, ISBN 978-92-64-99053-1, 2008.
- [8] http://www.cern.ch/n_TOF/n_TOF-ND-ADS/.
- [9] IP-EUROTRANS: European Research Program for Transmutation of High Level Nuclear Waste in Accelerator Driven Systems, FIGW-CT-2004-516520 nuklear-server.ka.fzk.de/eurotrans>.
- [10] M.C. Moxon, E.R. Rae, Nucl. Instr. and Meth. A 24 (1963) 445.
- [11] R.L. Macklin, J.H. Gibbons, Phys. Rev. 159 (1967) 1007.
- [12] J.L. Tain, et al., J. Nucl. Sci. Tech. 689 (Suppl. 2) (2002).
- [13] A. Borella, et al., Nucl. Instr. and Meth. A 577 (2007) 626.
- [14] <http://www.phy.ornl.gov/nuclear/orela/>.
- [15] N. Yamamuro, T. Doi, T. Miyagawa, Y. Fujita, K. Kobayashi, R.C. Block, J. Nucl. Sci. Tech. 15 (1978) 637.
- [16] C. Guerrero, et al., Application of photon strength functions to (n, γ) measurements with the n_TOF TAC, in: Proceedings of the Workshop on Photon Strength Functions and Related Topics, June 17–20, 2007, Prague, CZ, PoS(PSF07)006.
- [17] The n_TOF Collaboration, Measurement of the neutron capture cross-sections of ^{233}U , $^{240,242}\text{Pu}$, $^{241,243}\text{Am}$ and ^{245}Cm with a Total Absorption Calorimeter at n_TOF, INTC-2003-036, 2003.
- [18] M. Koizumi, et al., Nucl. Instr. and Meth. A 562 (2006) 767.
- [19] O. Scherbakov, K. Furutaka, S. Nakamura, H. Harada, K. Kobayashi, Nucl. Instr. and Meth. A 517 (2004) 269.
- [20] D.P. Barry, M.J. Trbovich, Y. Danon, R.C. Block, R.E. Slovacek, Nucl. Sci. Eng. 153 (2006) 8.
- [21] R. Reifarh, et al., Nucl. Instr. and Meth. B 241 (2005) 176.
- [22] S. Marrone, et al., Nucl. Instr. and Meth. A 517 (2004) 389.
- [23] L. Tassan-Got, et al., Fission of actinides induced by neutrons at n_TOF, in: AIP Conference Proceedings on Nuclear Data for Science and Technology, vol. 769, AIP, Melville, 2004, p. 1529.
- [24] M. Calviani, et al., Measurement of neutron induced fission of ^{235}U , ^{233}U and ^{245}Cm with the FIC detector at the CERN n_TOF facility, in: Proceedings of the International Conference on Nuclear Data for Science and Technology, vol. 750, Nice, France, 2007.
- [25] R. Plag, et al., Nucl. Instr. and Meth. A 496 (2003) 425.
- [26] F. Gunsing, et al., Nucl. Instr. and Meth. B 261 (2007) 925.
- [27] K. Wisshak, et al., Nucl. Instr. and Meth. A 292 (1990) 595.
- [28] M. Heil, et al., The Total Absorption Calorimeter of the n_TOF Collaboration, CERN n_TOF Report (ID: 250), February 2005. Available online from: www.cern.ch/ntof.
- [29] I. Dillmann, et al., The neutron absorber for the n_TOF TAC, n_TOF Internal Note, 2004.
- [30] D. Cano-Ott, et al., Monte Carlo simulation of the 4π Total Absorption Calorimeter at n_TOF, n_TOF Internal Report, 2003.
- [31] U. Abbondanno, et al., Nucl. Instr. and Meth. A 538 (2005) 692.
- [32] <http://www.acqiris.com>.
- [33] <http://castor.web.cern.ch/castor>.
- [34] E. Berthoumieux, Preliminary report on BaF₂ Total Absorption Calorimeter test measurement, Rap. Tech., CEA-Saclay/DAPNIA/SPhN, 2004.
- [35] D. Cano-Ott, et al., The n_TOF Collaboration, Measurements at n_TOF of the neutron capture cross section of minor actinides relevant to the nuclear waste transmutation, in: International Conference on Nuclear Data for Science and Technology, Santa Fe, USA, AIP Conference Proceedings, vol. 769, 2005, p. 1442.
- [36] C. Guerrero, et al., A Monte Carlo based dead-time correction method for measurements in coincidence, to be submitted.
- [37] C. Coceva, et al., Nucl. Instr. and Meth. A 489 (2002) 346.
- [38] A. Mengoni, et al., The n_TOF Collaboration, The physics case and the related proposal for measurements at the CERN neutron time-of-flight facility n_TOF in the period 2006–2010 (the n_TOF phase-2 initiative), CERN-INTC-2005-021, 2005.
- [39] R. Macklin, J. Halperin, R. Winters, Nucl. Instr. and Meth. A 164 (1979) 213.
- [40] C. Domingo, et al., Phys. Rev. C 75 (2007) 015806.
- [41] N.M. Larson, Updated users' guide for SAMMY: multilevel R-matrix fits to neutron data using Bayes' equations, ORNL/TM-9179/R6, 2003.
- [42] The Joint Evaluated Fission and Fusion File (JEFF-3.1) <http://www.nea.fr/html/dbdata/JEFF/>.
- [43] J. Pancin, et al., Nucl. Instr. and Meth. A 524 (2004) 102.
- [44] S.F. Mughabghab, Neutron Cross Sections, Academic Press, New York, 1984.
- [45] C. Guerrero, et al., Measurement at n_TOF of the $^{237}\text{Np}(n, \gamma)$ and $^{240}\text{Pu}(n, \gamma)$ cross-sections for the transmutation of nuclear waste, in: Proceedings of PHYSOR-2006, ANS Topical Meeting on Reactor Physics, Vancouver, Canada, September 10–14, 2006.
- [46] C. Guerrero, et al., Monte Carlo simulation of the n_TOF Total Absorption Calorimeter, to be submitted.
- [47] P.E. Koehler, et al., Phys. Rev. C 62 (2000) 055803-1.
- [48] M.C. Moxon, REFIT, A least square fitting program for resonance analysis of neutron transmission and capture data, Technical Report, AEA Industrial Technology, Harwell laboratory AEA-InTec-0470, 1991.
- [49] B.J. Allen, A.R. Musgrove, R.L. Macklin, Neutron sensitivity of capture gamma ray detectors, in: Proceedings of a Specialists' Meeting on Neutron Data of Structural Materials for Fast Reactors, Geel, Belgium, 1977, pp. 506–529.
- [50] K. Wisshak, et al., Phys. Rev. C 52 (1995) 2762.